Fermilab IOTA/FAST Experiment Proposal — August 30, 2022

Measurement of Coherence Length in UndulAtor RAdiation (CLARA): Run 4 Proposal

Sergei Nagaitsev*

Fermi National Accelerator Laboratory and the University of Chicago

Jonathan Jarvis, Aleksandr Romanov,† Alexander Shemyakin, Giulio Stancari, and Alexander Valishev

Fermi National Accelerator Laboratory

Ihar Lobach

Argonne National Laboratory

I. PURPOSE AND METHODS

The goal of the proposed experimental research is to investigate the quantum nature of "a particle in a ring" by studying a single 135-MeV electron, circulating in the IOTA storage ring and interacting with an undulator through single- and multi-photon emissions. The focus of this proposal will be two-photon undulator emissions.

The proposed experiment involves Mach-Zehnder (MZ) interferometry of the undulator radiation in IOTA, see Fig. 1. In this experiment, the pulse of radiation in one branch of the interferometer is delayed by a certain optical delay. In Fig. 1 we use a double wedge for illustration. Then, the two pulses pass through the second beam splitter. The optical delay can be adjusted with a step as small as 10 nm. It can be shown that when the optical delay is adjusted, we will observe oscillations of intensity in the two outputs of the interferometer, see [1] for example. This interference pattern contains information about the temporal shape of the undulator radiation pulse, also known as the radiation coherence length [2, p. 26]. The predicted coherence length is about 30 fs long. We propose to measure this coherence length in both multi-electron and single-electron regimes.

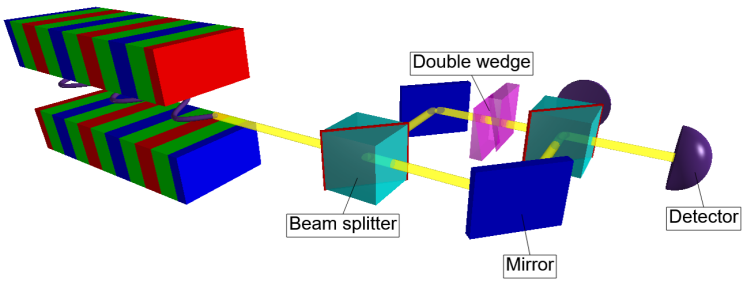

FIG. 1. Mach-Zehnder interferometry of undulator radiation.

The proposed experiment is an extension of the study of photon statistics of the undulator radiation, generated by a single electron, circulating in a storage ring [3–5], which took place during Run 2b and Run 3 of IOTA. In these previous experiments, we mostly used one binary Single Photon Avalanche Diode (SPAD)

* Principal Investigator; email: nsergei@fnal.gov; phone: (630) 840-4397
† Fermilab Liaison; aromanov@fnal.gov

detector (see [3]), i.e., it provided only two possible outputs per IOTA revolution: (1) no-detection, (2) detection. There was no photon number resolution. Only brief tests were carried out with two SPAD detectors. In this proposal, we describe a dedicated experiment where the undulator radiation is divided into two arms by an optical 50-50 beam splitter, and then it is detected by two SPAD detectors. Therefore, there will be three possible outcomes for each IOTA revolution: (1) no-detection, (2) detection in one of the SPADs, (3) detections in both SPADs.

Further, since we will record detection events for each detector individually, we will also be able to see if there is any correlation (or anticorrelation) between the detection events in the two SPADs. The electron in IOTA is believed to be a classical electric current (negligible electron recoil during radiation), which means that the radiation field should be in a coherent state (classical state) [6–8]. In this case, the coincidence detection rate should exhibit fast oscillations with changing the delay between two MZ interferometer arms with the coincidence probability equal to the product of probabilities of detecting individual photons. It is the intent of this experiment to determine if this is actually the case, because if the undulator radiation from a single electron in IOTA deviates from the expected coherent state, then the coincidence rate would deviate from the individual probabilities product. The ultimate case of such a deviation is photon wave packets in number (Fock) photon states, where the photon detection events are fully correlated, and the fast oscillations of the coincidence rate vs delay in the MZI arms are replaced by a smooth, Gaussian-like curve [9], known as "Hong-Ou-Mandel (HOM) dip." We may also test if the single-electron undulator radiation is a mixture of pure-classical and Fock states and try to establish an upper limit for the contribution of the latter.

II. BEAM CONDITIONS

We request a focusing lattice in the IOTA ring with good life time at small beam currents (> 30 min, but preferably even longer, ≈ 2 hr). The rms bunch length should be about 30 cm. It can be shorter, but it does not have to be. The SLAC undulator will be in the "in" position (the perturbation in beta functions introduced by the undulator is negligible). The transverse beam size in the undulator should not exceed about 1–1.5 mm, but the exact value does not matter. We would recommend to place a minimum of beta functions at the center of the undulator, and to minimize dispersion in the undulator, which is the standard practice for experiments with undulator radiation. However, it is not required for the proposed single-electron experiments, as long as the beam size requirement is met. Our studies will be conducted in the following three regimes:

- Single electron circulating in the ring for a long time (> 30 min).
- Small number of electrons circulating in the ring, 1-1000. Preferably, all in one bucket.
- Nominal IOTA beam current (≈ 2 mA)

The beam energy 135 MeV is requested for our studies in order to attain the 630-nm wavelength for the fundamental of the undulator radiation.

III. APPARATUS

A. Layout

The CLARA apparatus consists of the Mach-Zehnder Interferometer (MZI) with associated optics as well as Single Photon Avalanche Diodes (SPADs) and a digital camera (DC). The schematic of the apparatus to be installed at IOTA is shown in Fig. 2.

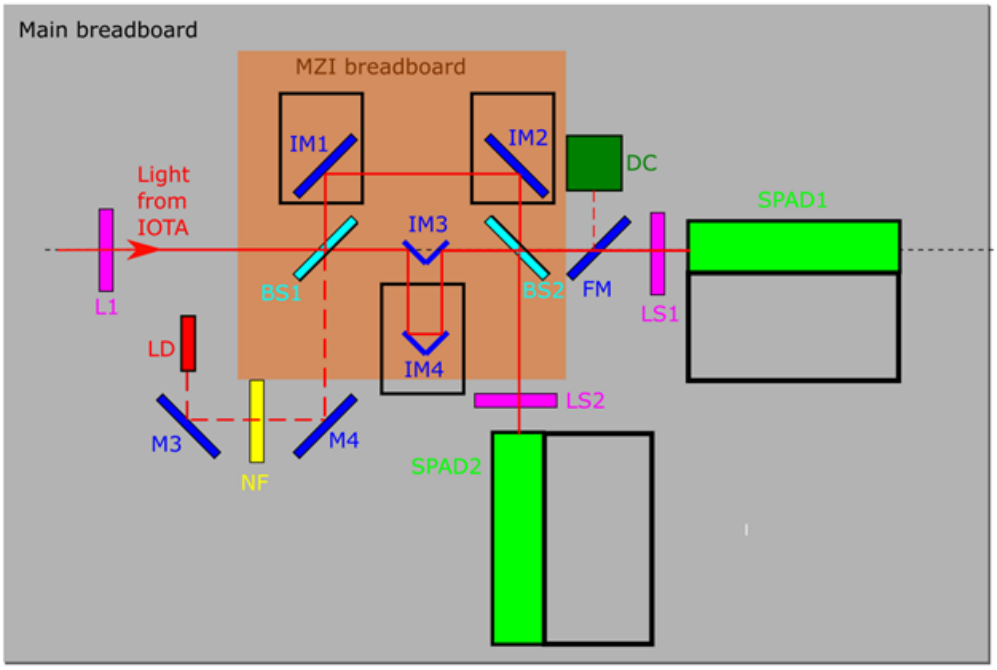

FIG. 2. Schematic of the apparatus to be installed at IOTA. L1, LS1, LS2 – lenses. M3, M4, IM1, IM2 – mirrors. FM – flipping mirror. BS1, BS2 – beam spitters. DC – digital camera. SPAD1, SPAD2 – SPADs. LD – laser diode used for MZI tuning. NDF – neutral density filter.

The equipment shown in Fig. 2, assembled in an optical box, will be installed on the top of the M4R dipole magnet. The light generated by the SLAC undulator will pass through the bend, exit the vacuum chamber through a vacuum window, and be directed by two existing remotely controlled mirrors, M1 and M2 (not shown), into the optical box. In the box, the light beam is focused by the lens L1 and enters the MZI through the beam splitter BS1. In the MZI, the photons may follow two paths. In the first case, they are reflected from BS1, mirrors IM1, IM2, and arrive to the beam splitter BS2. In the second case, photons pass BS1, go between right-angle mirror IM3 and hollow-roof mirror IM4, and come to BS2. The distance between IM3 and IM4 can be adjusted with 25 nm steps using the stage on which IM4 is mounted. The elements of the MZI are assembled on a separate optical breadboard, isolated by dampers from the main board to decrease vibrations.

To test MZI tuning without IOTA beam, a Laser Diode LD is installed within the same optical box. Its light is directed into the second MZI input port at BS1 with mirrors M3 and M4. To mimic measurements with single photons, a neutral density filter, NDF, can be installed on the LD light path.

Depending on the final results of tests at ESB, an additional low-attenuation neutral filter might be installed in the MZI to compensate for unequal reflection losses in the MZI arms. Also, an additional bandpass filter might be installed at the entrance of the box (at L1 location).

B. Controls and Data Acquisition

The main components of the controls data acquisition system are listed below.

1. 3D positions of each SPAD and their shutters are remotely controlled.
2. The angular positions of M1, M2, BS2 and IM1 are remotely adjustable in two planes.
3. The hollow-roof mirror IM4 is mounted on a remotely controlled precision stage with 25 nm steps.
4. Position of the flipping mirror is controlled remotely through the provided controller.
5. The laser diode can be turned on/off remotely.
6. The signal from the DC is processed with the standard IOTA program for image processing.
7. Signals from the SPADs are sent to discriminators and coincidence units and delivered to the ACNET counters and to the picosecond event timer (Picoquant HydraHarp 400).

Items 1–5 are controlled by Raspberry Pi front-end computers.

C. Data Storage, Analysis and Documentation

Data will be saved on the IOTA/FAST network drive (iota-fast.bd), with at least one backup copy on another Fermilab machine. Analysis scripts and reports will be archived in a code repository on Fermi Redmine and on Github or Bitbucket. The experiment wiki page will be hosted on Fermi Redmine.

IV. EXPERIMENTAL RUN PLAN

A. Stages of the Experiment

The experiment will be performed in the following stages, described in the following sections.

1. Assembly and tests at ESB
2. Transport of the optical box into IOTA enclosure, mounting, connecting and light tightening
3. Testing and tuning with the laser diode using CCD
4. Measurement of the coherence length of the undulator light for a large electron bunch population
5. Remote re-tuning of MZI for measurements with SPADs using the laser diode
6. Measurements with a single electron
7. Disassembly
8. Offline analysis

B. Tests at ESB

Assembly and most of preliminary tuning are being made at the ESB test stand. The present configuration of the optical box is shown in Fig. 3. At the end of these tests we expect the following:

1. All components will be assembled, aligned, and tested.
2. Remote operation will be established.
3. Interference pattern of the light from the laser diode will be established and recorded with the DC.
4. The scheme with SPADs recording a highly attenuated light from the laser diode will be established. Signal from SPADs will be recorded, and their dependence on the MZI delay will be analyzed.
5. Procedure of tuning for the DC/SPADs modes will be developed and documented.
6. The optical box will be prepared for transportation into IOTA and mounting.

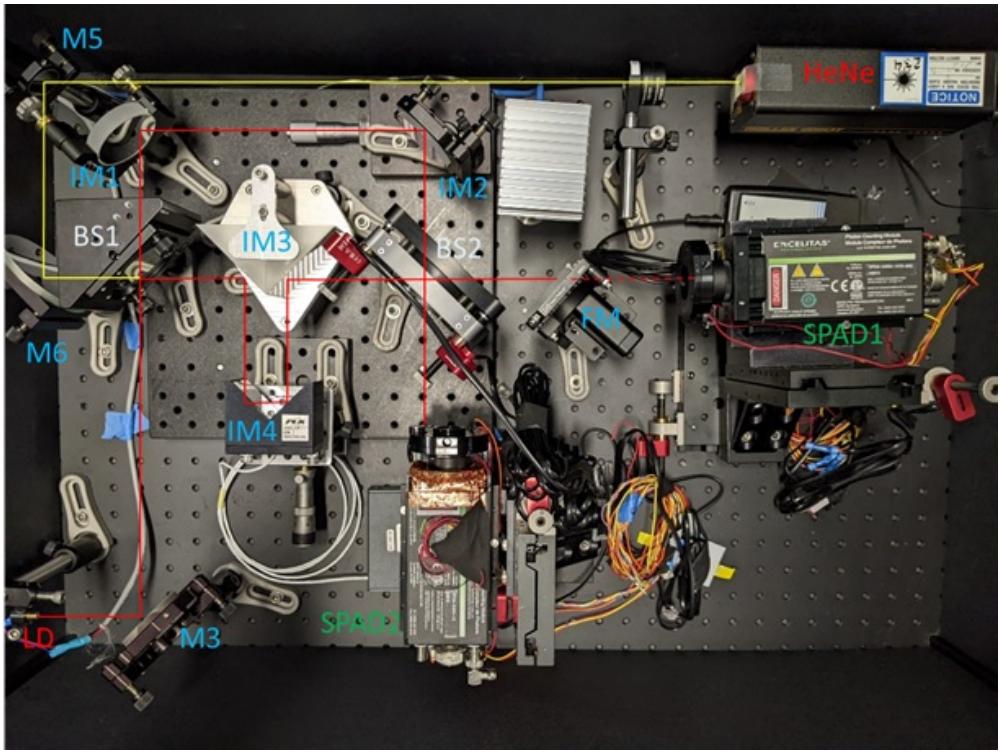

FIG. 3. Photo of the optical box at the ESB test stand. L1, LS1, LS2 – lenses. M3, M4, IM1, IM2 – mirrors. FM – flipping mirror. BS1, BS2 – beam spitters. DC – digital camera. SPAD1, SPAD2 – SPADs. LD – laser diode used for MZI tuning. NDF – neutral density filter. Lenses are not installed yet. Initial alignment is performed with HeNe laser (HeNe; will be removed in the final configuration). Its light is guided into MZI by mirrors M5 and M6.

C. Transport to the IOTA Enclosure

The optical box with an attached chassis will be transported as a unit into the IOTA enclosure using manual carts and the elevator. It will be mounted on the top of the M4R dipole magnet.

D. Measurements with Many Electrons

Measurements of the coherence length in the case of a large electron bunch population is made with a digital camera. The flipping mirror FM is inserted to reflect the beam into the DC. The BS2 is misaligned so that the light beams coming through two MZI arms create an interference pattern at a CCD with multiple fringes over the image. The spatial wavelength λ_{sp} of the pattern is determined by the angle α_0 between wavefronts of the light coming to CCD from two MZI arms:

$$\lambda_{sp} = \frac{\lambda_0}{\alpha_0}, \tag{1}$$

where λ_0 is the central wavelength of the light. An example of the expected pattern simulated with SRW is shown in Fig. 4.

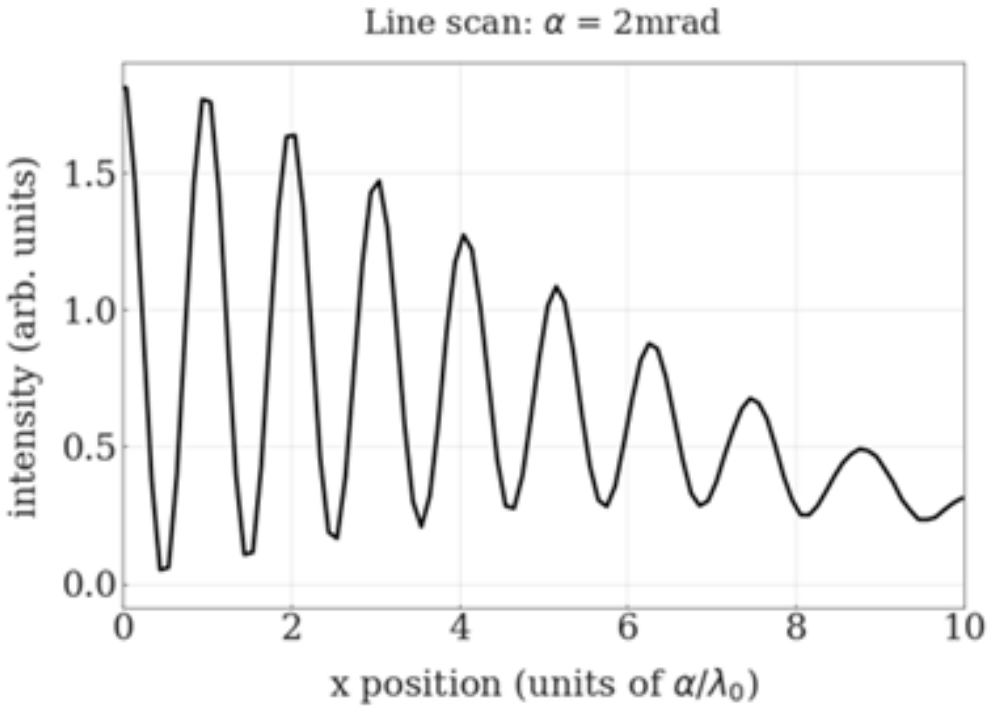

FIG. 4. An SRW simulation of the interference pattern at DC with the BS2 misalignment of 2 mrad and a perfect overlap of images from two MZI arms.

To observe the interference pattern similar to Fig. 4, the following three conditions should be met.

1. For an optimum measurement, the entire pattern (about 20 oscillations) should fit into the DC aperture of about 10 mm. For $\lambda_0 = 630$ nm, it implies $\alpha_0 = 1$ mrad. The most likely scenario is that the angle is misaligned in the horizontal plane and is well aligned in the vertical plane.

2. The images created at DC by light passing through two MZI arms should overlap.

3. The length of two MZI arms is the same to within one wavelength λ_0.

To satisfy these conditions, angles of IM1 and BS2 as well as the MZI delay (difference between the arms' lengths) need to be adjusted. Both α_0 and images overlap are affected by the difference IM1 and BS2 angles. However, the distance from IM1 to CCD is approximately a factor of two larger than the one from BS2 to CCD. Therefore, if they are adjusted simultaneously but with IM1 changing by half of the BS2 change, the overlap is preserved. When the first two conditions are satisfied, the delay is scanned using the IM4 stage until the interference pattern appears.

The procedure has been tested with a Laser Diode at ESB; see Fig. 4 for an example of the observed interference pattern.

The optical box is expected to arrive to the IOTA enclosure at the state tuned for this measurement. The first step will be to check the MZI alignment with the LD and, likely, to carry out minor adjustments to compensate for the shifts during transportation.

Then, the undulator light is directed into the MZI using fine tuning of the mirrors M1, M2.

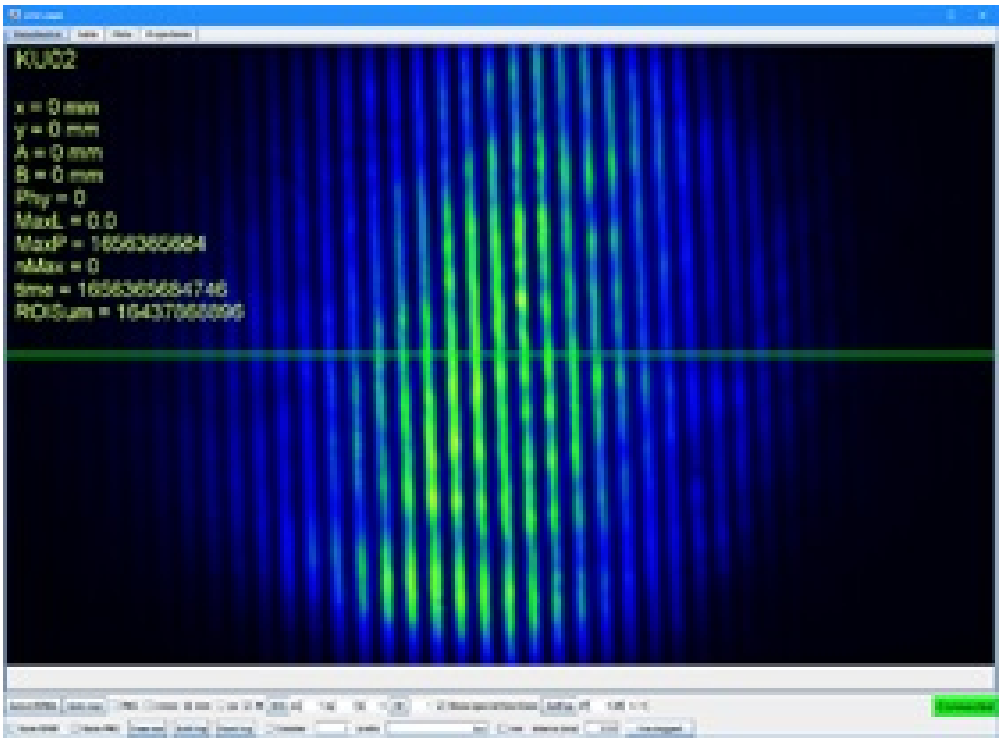

FIG. 5. The interference pattern for the light from a Laser Diode, observed at the ESB test stand with DC.

Finally, the measurements are performed at the optimum beam energy of 135 MeV. DC images are recorded at several bunch intensities.

E. Re-tuning for Measurements with Single Electrons

To transition to measurements with a single electron (and, correspondingly, single or double photons), the MZI is tuned into the position of the best possible alignment. In terms of Fig. 4, this state corresponds to the wavelength of spatial oscillation being much larger than the DC image size. Depending on the delay in the MZI, the image might be a bright, dark, or gray spot.

The transition is made using the LD light. It begins by decreasing of misalignment angles in IM1 and BS2 while observing with the DC an increase of the spatial wavelength and adjusting the delay as required. When the spatial wavelength is larger than the DC active area, tuning begins to rely on the total intensity of the light coming to DC measured as a function of the position of the IM4 stage. The curve simulated for the ideal alignment in the case of the undulator light is shown in Fig. 6. Note that the details of the curve depend on the bandwidth of the system (e.g. applied optical filters) and aperture restrictions, which will be determined during the experiments.

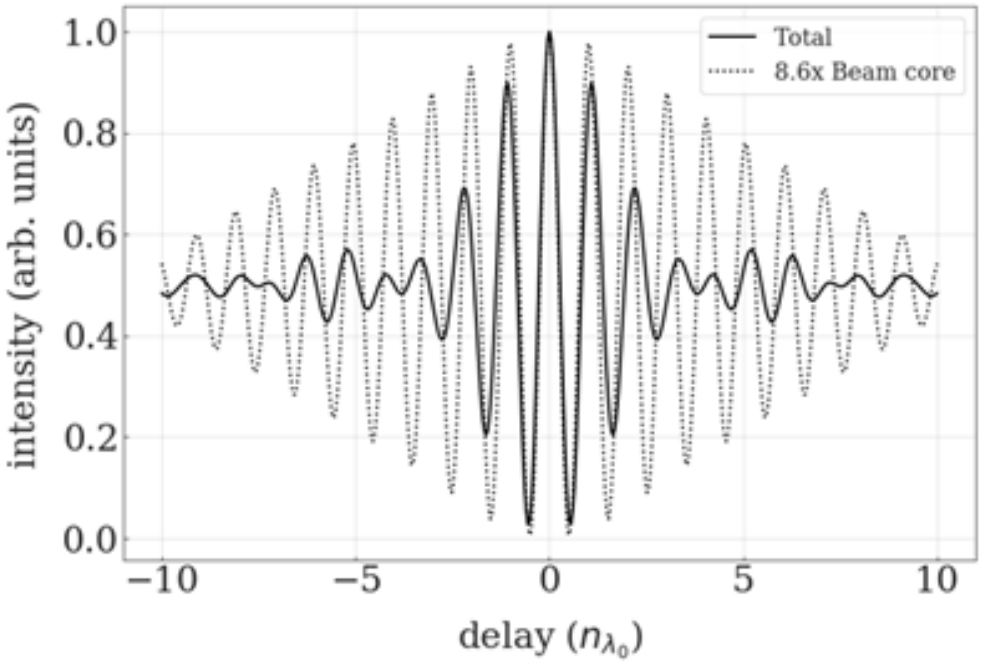

FIG. 6. Intensity at one of the IB2 ports as a function of the delay between arms.

The best alignment corresponds to the largest visibility V of the curve defined as

$$V = \frac{I_{max} - I_{min}}{I_{max} + I_{min}}, \tag{2}$$

where I_{max} and I_{min} are neighboring maximum and minimum of intensity. While one of the goals of the experiment is to measure how the visibility changes with the delay to characterize the undulator light properties, visibility at the image center is defined mainly by quality of the MZI alignment independently of the source of light. It justifies using the LD for MZI tuning described in this section. The final state of the MZI at this stage is a maximum intensity coming out of one BS2 port (e.g. toward SPAD1) and a minimum intensity in the other one.

After finishing this tuning, the neutral density filter NDF in Fig. 2 is installed, the flipping mirror FM is retracted, and SPAD shutters are open. During the test at ESB, attenuation of this filter will be chosen to pass into the MZI the light with intensity not damaging the SPADs. Also during these tests, the SPADs will be roughly aligned so that the light beam comes to the center of the DC with the flipping mirror FM inserted and goes to the center of SPADs with the FM removed from the light path. Therefore, only minor adjustments are expected to be required to account for shifting during transport. They will be made based on dependencies of the SPAD's photon count of SPAD position.

F. Single-Electron Measurements

To compare as close as possible single-electron results with multi-electron case, the first step of the measurement is to record the total intensity of the DC images as a function of the MZI delay at the best MZI alignment described in the previous section. The SPADs' shutters are closed, the flipping mirror is moved in, and the undulator light from the multi-electron bunch at the optimal energy (135 MeV) is centered at DC with the MZI delay corresponding to the bright spot at DC. The total DC image intensity is recorded as the IM4 stage moves by 25 nm steps for the total travel of about ten $\lambda_0 \approx 7$ μm for several times in both directions. Since the CCD numbers are recorded asynchronously with the stage positions, the analysis will rely on finding the corresponding pattern in the CCD data. We are working on options to record the stage positions in ACNET.

We will then re-establish the procedures used in Run 2 and Run 3 to obtain a few electrons circulating in IOTA by injecting dark current and by scraping with with rf-voltage reduction. We will also make sure that we can reliably determine the number of electrons in the ring using the signals from PMTs and synclight cameras. Initial rough alignment of the SPADs can be performed by looking at the light spots (produced by nominal beam current) on the closed optical shutters of the SPADs. Then, fine alignment of the SPADs with 100–1000 electrons can be performed. The optimal positions of the SPADs will be found by scanning the photocount rates along x, y, z directions and finding the maxima, iteratively. A data set with zero electrons should be collected to verify the dark counts of the two SPADs.

Next, a single electron is stored in IOTA. The SPADs' shutters are opened, and the flipping mirror is removed. SPAD position scans are performed to verify that the alignment found with LD is still valid.

The main measurement consists of recording SPAD counts as a function of the IM4 stage position in the same pattern as for the case of the multi-electron measurements, except for the longer time at each step. The measurement might be repeated with different filtering. As in the multi-electron case, the SPAD counting may be recorded asynchronously with the stage motion, so the correspondence needs to be reconstructed by finding the pattern in the SPAD data. Coincidence rates will be available online through the ACNET counters. They will also be reconstructed offline from the event timer time stamps.

G. Installation, Commissioning and Beam Time Requests

The experiment stages and the estimated time required for each of them are summarized below. Shifts should be separated in time by several days for preliminary analysis and adjustments.

Installation		
Installation in IOTA tunnel at M4R. Mounting, connecting and initial testing.	(access)	2×8 h
Experiments at high bunch intensity		
Commissioning with laser diode.	(no beam)	3×4 h
Commissioning of 135-MeV beam. Optional energy scan to maximize signal.		2×8 h
MZI measurements.		4×8 h
Transition to few electrons		
Alignment of camera and SPADs with laser diode and delay scans.	(no beam)	4×8 h
Experiments with few and single electrons		
Re-establish procedures for injection, scraping, electron counting.		2×8 h
MZI data collection with 0, 1 and 2 electrons.		4×8 h

V. PERSONNEL ROLES

Jonathan Jarvis: methodology, investigation, software, validation, writing

Ihar Lobach: conceptualization, investigation, software, writing

Sergei Nagaitsev: conceptualization, methodology, funding acquisition, project administration, resources, supervision, writing

Aleksandr Romanov: conceptualization, methodology, data curation, formal analysis, investigation, resources, software, validation, writing

Alexander Shemyakin: conceptualization, methodology, investigation, resources, writing

Giulio Stancari: conceptualization, methodology, data curation, formal analysis, investigation, resources, software, writing

Alexander Valishev: funding acquisition, project administration, supervision

(See also credit.niso.org.)

VI. FUNDING

The project is funded by a Fermilab LDRD grant [10].

VII. ACKNOWLEDGEMENTS

This manuscript has been authored by Fermi Research Alliance, LLC under Contract No. DE-AC02-07CH11359 with the U.S. Department of Energy, Office of Science, Office of High Energy Physics.

---

[1] P. Grangier, G. Roger, and A. Aspect, Experimental evidence for a photon anticorrelation effect on a beam splitter: A new light on single-photon interferences, EPL (Europhysics Letters) **1**, 173 (1986).

[2] K.-J. Kim, Z. Huang, and R. Lindberg, *Synchrotron Radiation and Free-Electron Lasers* (Cambridge University Press, 2017).

[3] URSSE Run 2 proposal, `https://cdcvs.fnal.gov/redmine/attachments/57543/Lobach_URSSE_Proposal_2019-12-12_v1.pdf` (2019), accessed: 2020-10-06.

[4] I. Lobach, S. Nagaitsev, and G. Stancari, *Measurement of Spontaneous Undulator Radiation Statistics Generated by a Single Electron (URSSE)*, Tech. Rep. FERMILAB-FN-1115-AD (Fermilab).

[5] I. Lobach, *Statistical Properties of Undulator Radiation: Classical and Quantum Effects*, Ph.D. thesis, University of Chicago (2021), FERMILAB-THESIS-2021-27.

[6] R. J. Glauber, Some notes on multiple-boson processes, Phys. Rev. **84**, 395 (1951).

[7] R. J. Glauber, Coherent and incoherent states of the radiation field, Phys. Rev. **131**, 2766 (1963).

[8] R. J. Glauber, The quantum theory of optical coherence, Phys. Rev. **130**, 2529 (1963).

[9] C. K. Hong, Z. Y. Ou, and L. Mandel, Measurement of subpicosecond time intervals between two photons by interference, Phys. Rev. Lett. **59**, 2044 (1987).

[10] S. Nagaitsev, I. Lobach, A. Romanov, and G. Stancari, Quantum effects in undulator radiation (2019), Fermilab LDRD Grant no. L2019.025, June 2019 – March 2023.